

CHAPTER

The Stress of Misfolded Proteins: *C. elegans* Models for Neurodegenerative Disease and Aging

Heather R. Brignull, James F. Morley and Richard I. Morimoto*

Abstract

A growing number of human neurodegenerative diseases are associated with the expression of misfolded proteins that oligomerize and form aggregate structures. Over time, accumulation of misfolded proteins leads to the disruption of cellular protein folding homeostasis and eventually to cellular dysfunction and death. To investigate the relationship between misfolded proteins, neuropathology and aging, we have developed models utilizing the nematode *C. elegans*. In addition to being genetically tractable, *C. elegans* have rapid growth rates and short life-cycles, providing unique advantages for modeling neurodegenerative diseases of aging caused by the stress of misfolded proteins. The *C. elegans* models described here express polyglutamine expansion-containing proteins, as occur in Huntington's Disease. Through the use of tissue-specific expression of different lengths of fluorescently tagged polyglutamine repeats, we have examined the dynamics of aggregate formation both within individual cells and over time throughout the lifetime of individual animals, identifying aging and other genetic modifiers as an important physiologic determinant of aggregation and toxicity.

Introduction

Misfolded proteins, aggregates, and inclusion bodies are hallmarks of a range of neurodegenerative disorders including Alzheimer's disease (AD), Parkinson's disease (PD), prion disorders, amyotrophic lateral sclerosis (ALS), and polyglutamine (polyQ) diseases that include Huntington's disease (HD) and related ataxias.¹⁻³ Each of these disorders exhibits aging-dependent onset and selective neuronal vulnerability despite widespread expression of the related proteins, and a progressive, usually fatal clinical course. The deposition of intra- or extracellular protein aggregates is a well-conserved pathological feature and has been the focus of extensive investigation.⁵ Despite differences in the underlying genes involved, inheritance and clinical presentation, the similarities observed have led to the proposal of shared pathogenic mechanisms and the hope that insights into one process may be generalized to others.

In support of this premise is growing evidence that the cellular protein quality control system appears to be an underlying common denominator of these diseases.⁴ For example, genes involved in protein folding and degradation, including molecular chaperones and components of the proteasome, have been shown to modulate onset, development and progression in models of multiple neurodegenerative diseases.⁵⁻⁷ Further, it has been suggested that despite

*Corresponding Author: Richard I. Morimoto—Department of Biochemistry, Molecular Biology, and Cell Biology. Rice Institute for Biomedical Research, Northwestern University, 2153 North Campus Drive, Evanston, Illinois 60208, U.S.A. Email: r-morimoto@northwestern.edu

the absence of sequence homology, different disease-related proteins share a common ability to adopt similar proteotoxic conformations and that these might be used as therapeutic targets.^{8,9}

Models of Neurodegenerative Disease

Some of these disorders, including the polyQ diseases, exhibit familial inheritance, allowing the use of genetic studies and positional cloning to identify single gene alterations underlying the disorders.¹⁰⁻¹³ Other diseases are sporadic, but rare familial forms have allowed the identification of candidate genes that could reveal insights into pathology. These include mutations of amyloid precursor protein in AD, parkin and α -synuclein in PD and superoxide dismutase in ALS.¹⁴⁻¹⁹ Identification of these genes has led to the development of many model systems to investigate the underlying pathology and to identify factors and pathways that modify the disease process.

In addition to transgenic mouse and cell culture models has been the development of invertebrate models using *Drosophila* and *C. elegans* for the study of neurodegenerative disease.²⁰⁻²⁴ As described here for *C. elegans*, these systems provide a genetic approach for identification of modifiers of both cellular and behavioral phenotypes which together with a relative ease of technical manipulation facilitates rapid, high-throughput testing of hypotheses.

In a number of cases, disease gene orthologs have been identified and their loss of function phenotypes observed. For example, inactivation of the fly *parkin* gene results in a degenerative phenotype.^{25,26} However, pathogenic mechanisms in neurodegeneration often involve a gain of function toxicity allowing these disorders to be modeled using transgenic overexpression of human disease-related proteins regardless of whether a clear ortholog can be identified. Expression of polyQ containing proteins is neurotoxic in both *Drosophila* retinal neurons and *C. elegans* chemosensory or mechanosensory neurons despite the absence of clear disease gene orthologs.²⁷⁻³⁰ Similar strategies have been used to examine the toxicity of APP, SOD, α -synuclein in flies and worms.^{21,31-36} Despite the idiosyncrasies of different models, each provides unique insights that clearly validate the general approach.

C. elegans Model of polyQ Disease

Our studies have focused initially on polyQ expansions as occur in Huntington's Disease and related disorders including several spinocerebellar ataxias and Kennedy's Disease.³⁷⁻⁴⁰ At least nine human neurodegenerative diseases are associated with polyQ expansions within otherwise unrelated genes. In addition to a shared pathogenic motif, gene products associated with this class of neurodegenerative diseases are ubiquitously expressed but affect only neurons. Even within neuronal tissues, diseases show subset-specific aggregation, toxicity, and death.^{40,41}

Expression of expanded polyQ, with or without flanking sequences from the endogenous proteins—or when inserted into an unrelated protein—is sufficient to recapitulate pathological features of the diseases in multiple model systems including the appearance of protein aggregates, loss of cell function, and cell death.^{40,42-45} This suggests a central role for the polyQ expansion in these disorders and supports an approach whereby expression of isolated polyQ expansions without flanking sequences could lend insight into shared features of these disorders.

In vivo, pathogenesis is length-dependent and results from a toxic gain of function.^{37,40,46,47} Genetic studies have established that Huntingtin alleles from normal chromosomes contain fewer than 30-34 CAG repeats, whereas those from affected chromosomes contain greater than 35-40 repeats.⁴⁸ Analysis of patient databases has established a strong inverse correlation between repeat length and age of onset.^{48,49} Similar length dependencies are seen for the other polyQ repeat diseases suggesting a 35-40 residue threshold at which the disease gene products are converted to a proteotoxic state.

C. elegans, as a model has certain advantages for the study polyQ expansions. *C. elegans* is a roundworm that in its free-living form can be found in a variety of soil habitats. In the laboratory, the animals can be readily cultured in large numbers on agar plates seeded with a lawn of *E. coli*, as wild-type adult animals reach a maximum length of approximately 1mm.

The adult stage is preceded by progression through embryonic development, four stereotyped larval stages and an additional alternative quiescent form—termed the dauer larva—that can be accessed under conditions of low food, high population density or conditions otherwise unfavorable for growth. This life cycle is completed in approximately 2 days under typical growth conditions (20–25°C).

At all stages of development, *C. elegans* are transparent, permitting easy detection of fluorescent proteins in live animals. The hermaphrodite body plan is relatively simple, comprised of 959 somatic cells of which 302 cells are neurons. Despite the small number of cells *C. elegans* have multiple complex tissues types including intestine, muscle, hypodermis and a fully differentiated nervous system. Furthermore, *C. elegans* display conservation of basic molecular mechanisms enabling comparison with vertebrate models.^{50–52} Thus, despite its simplicity and ease of handling, studies in *C. elegans* can offer insight into processes unique to complex multicellular organisms.

The *C. elegans* polyQ Series in Neurons

To determine the effect of polyQ proteins in the neurons of *C. elegans*, we took a broad approach and expressed polyQ proteins throughout the nervous system. Phenotypes such as aggregation and neurotoxicity would therefore be the result of an integrated, system wide stress response rather than the stress response of a few isolated cells. Transgenic lines were generated using a range of polyQ expansion proteins (Q0, Q19, Q35, Q40, Q67, Q86) tagged with a fluorescent protein, and then expressed in neurons.

In young adult animals, expression of Q19 resulted in a pattern of diffuse neuronal distribution that persisted throughout the life of the animal, similar to control animals expressing the fluorescent marker (Q0). In Q19 animals cell bodies of commissural neurons (Fig. 1B, arrow) and the dorsal nerve cord (DNC) (Fig. 1B, open arrow), can be observed. The DNC is formed almost exclusively of neuronal processes and therefore displays a smooth, diffuse fluorescent intensity in Q19 animals. By comparison, the ventral nerve cord (VNC) contains visible cell bodies scattered along its length (Fig. 1B, triangle).

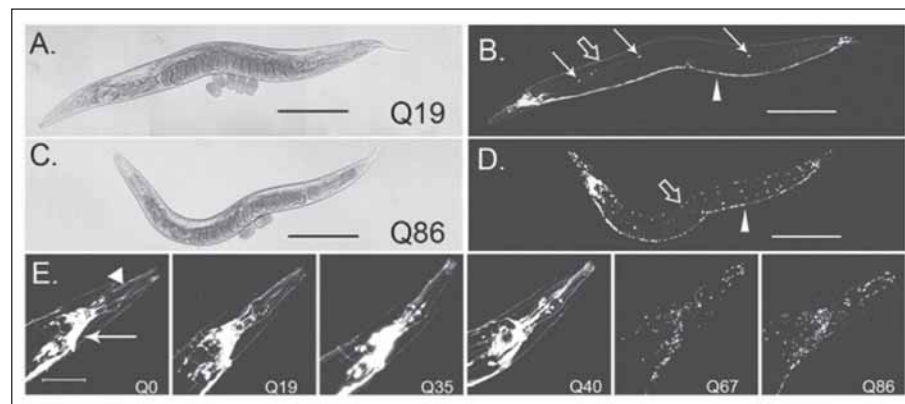


Figure 1. Poly-Q length dependent changes in protein distribution patterns. Pan-neuronal Q19::CFP has a soluble distribution pattern (A,B) while Q86::CFP is distributed into discrete foci (C,D). Arrows indicate commissural neurons. Open arrow indicates DNC, triangle indicates VNC, scale bar = 100 μ m. E) Flattened z-stacks of *C. elegans* head, scale bar = 50 μ m. Expressing a range of polyQ lengths reveals that proteins with tracts of \leq Q40 maintain a soluble distribution pattern while those \geq Q67 form foci. All animals depicted are young adults, four days post-hatch.

Distribution of Q86 protein was strikingly different from the diffuse distribution of Q19 protein. Throughout the nervous system, Q86 protein was limited to discrete foci, indicating polyQ length-dependent aggregation in *C. elegans* neurons (Fig. 1C-D). Q86 foci were detected in the earliest larval stage and persisted throughout the lifespan of the animal suggesting that length-dependent changes in distribution of proteins with long polyQ expansions occurred independent of neuronal subtype in *C. elegans*.

To determine the threshold length required to change the distribution pattern from diffuse (Q19) to foci (Q86), we expressed Q35, Q40, and Q67 fused to a fluorescent reporter. Animals expressing proteins with \leq Q40 display clearly delineated neuronal cell bodies and processes, suggesting the presence of soluble proteins. The soluble distribution pattern of Q0, Q19, Q35 and Q40 can be clearly observed in the head of *C. elegans* where the distinctive neuroanatomy of chemosensory processes (Fig. 1E, arrow) and the circumpharyngeal nerve ring can be identified (Fig. 1E, triangle). Q67 formed foci exclusively, similar to those observed in neurons of Q86 *C. elegans* (Fig. 1E). In contrast, the distribution pattern of proteins \leq Q40 never resembled that of Q67 or Q86. The polyQ length-dependent changes in protein distribution shown here, together with a threshold for foci formation of $>$ Q40, recapitulate two of the major features of most polyQ-repeat diseases.

Biophysical Properties of polyQ Proteins in Neurons of Live Animals

The soluble distribution pattern of protein with \leq Q40 was visually distinct from Q67 and Q86. To assess whether the visual changes in distribution correspond to changes in protein solubility, we employed fluorescence recovery after photobleaching (FRAP) analysis. Determining the rate of recovery after photobleaching in an individual neuron provides a direct measure of protein solubility and mobility and therefore enabled us to discriminate between changes in distribution due to protein aggregation, in which interacting proteins are stably associated and immobile, or changes due to restricted subcellular localization.^{53,54}

FRAP experiments on live animals that expressed a soluble control, Q0 or Q19, showed rapid recovery from photobleaching (Fig. 2A,B) consistent with soluble protein (Fig. 2D). However, foci bleached in Q86 neurons did not recover, indicating that the protein was immobile, from which we concluded that protein aggregates had formed (Fig. 2C,D). FRAP results were confirmed by Western blot analysis showing that Q86 aggregates were resistant to 5% SDS treatment, characteristic of polyQ aggregates.^{55,56} Therefore, aggregates in our analysis of *C. elegans* neurons were visually distinct foci formed by stably associated, immobile proteins. Q86 aggregates failed to recover from photobleaching in all neurons examined, a result which suggests that polyQ aggregates form independently of cell-type. This observation is consistent with the extensive distribution of Q86 proteins into foci as described (Fig. 1C-E).

It has been proposed that polyQ expansions result in the formation of β -sheet structures that self-associate and lead to aggregation.^{57,58} This hypothesis predicts that in addition to being immobile and resistant to SDS, polyQ proteins in aggregates would be closely associated in an ordered structure. Fluorescence Resonance Energy Transfer (FRET) is a technique developed for in vitro biochemical studies and applied to cell culture to determine in vivo, the proximity of two proteins. The resolution of this technique is in the nanometer range; FRET is maximal at 50Å and will not occur if proteins are more than 100Å apart. This technique has been widely employed to show protein interactions in vitro and in cell culture.^{59,60} We therefore performed FRET experiments to determine whether polyQ proteins in *C. elegans* neurons are sufficiently ordered, and in molecular proximity for energy transfer between CFP and YFP.

FRET efficiencies were determined for neurons of a live animal using the acceptor photobleaching technique in which donor (CFP) intensity is compared before and after acceptor (YFP) photobleaching.⁶¹ In *C. elegans* expressing both Q19::CFP and Q19::YFP, acceptor photobleaching had no effect on donor intensity, similar to negative control animals (Fig. 3C-F). These results show that, indirectly, FRET was not occurring between Q19 proteins. In contrast, FRET was observed in neuronal aggregates of expanded polyQ proteins. *C. elegans*

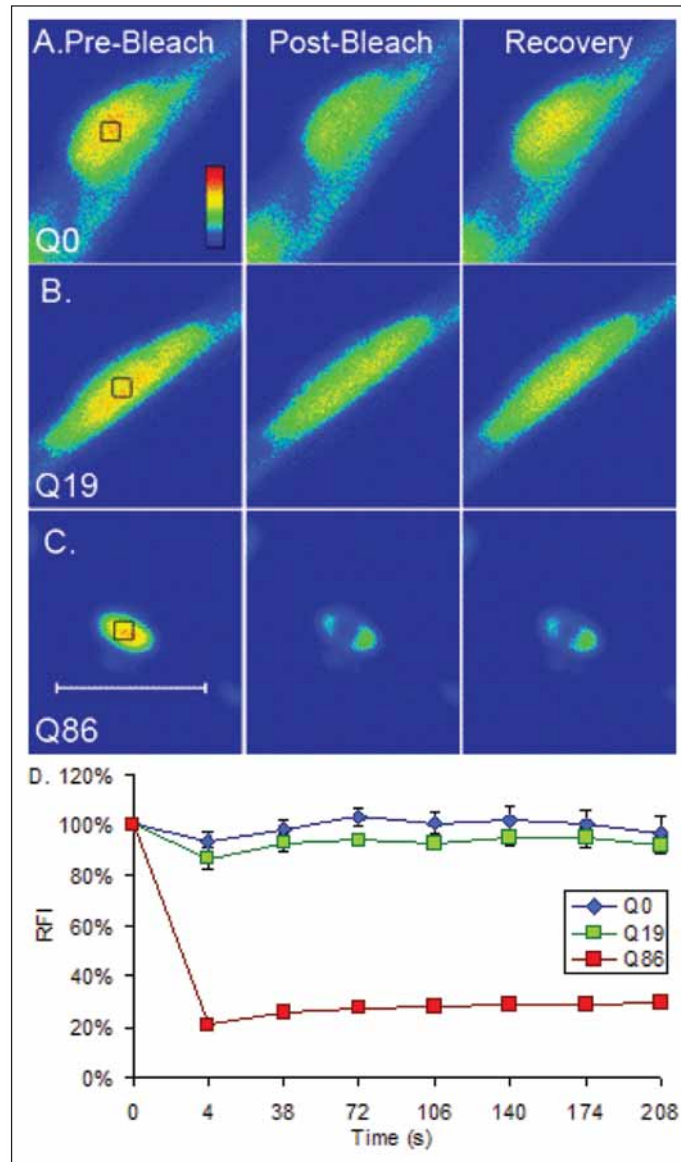


Figure 2. Solubility of PolyQ foci is consistent with aggregation. FRAP in *C. elegans* neurons expressing Q19::YFP, a photobleached area (box) recovers rapidly (B,D), similar to Q0 (A,D) indicating soluble proteins while bleached Q86::YFP foci do not recover (C,D). Therefore, Q86::YFP foci are insoluble, consistent with aggregation. Quantification (D) is ≥ 5 experiments with SEM. Signal intensity is measured in the color scale (A) where blue is least intense and red is most intense. Bar = 5 μm . A color version of this figure is available online at www.Eurekah.com.

coexpressing Q86::CFP and Q86::YFP showed an increase in donor intensity following acceptor photobleaching, similar to positive of animals expressing a chimeric protein of CFP linked to YFP (Fig. 3A-B,G-H).⁵⁹ FRET positive aggregates were detected in a wide range of neurons

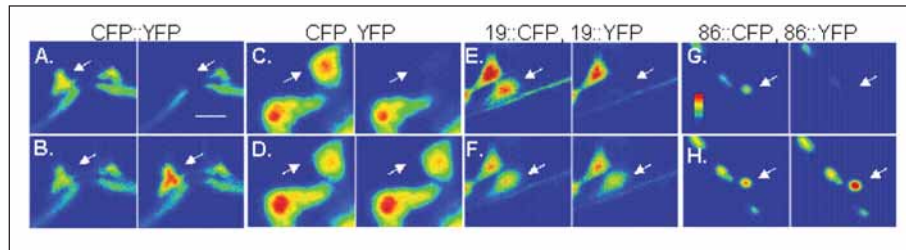


Figure 3. Q86 protein in neuronal aggregates exhibits FRET, indicating close and roughly ordered interactions at the molecular level. YFP photobleaching is seen on the YFP channel, (panels A,C,E,G) and its effect on CFP donor intensity in the same cell (panels B,D,F,H). Control animals expressing CFP::YFP FRET (A,B), $E_i = 0.248(\pm 0.089)$ while CFP and YFP coexpression (C,D) do not FRET, $E_i = 0.001(\pm 0.025)$. Neurons coexpressing Q19::CFP and Q19::YFP (E,F) do not FRET, $E_i = -0.090(\pm -0.057)$ while coexpression of Q86::CFP and Q86::YFP (G,H) does produce FRET, $E_i = 0.224(\pm 0.076)$. Cells shown are representative of FRET experiments. Intensity is by a color scale (G) where blue is least intense and red is most intense. Scale bar = 2 μm . A color version of this figure is available online at www.Eurekah.com.

with no clear correlation between FRET intensity and cell-type. The visible redistribution of Q67 and Q86 into foci, combined with SDS resistance, FRAP and FRET data, shows that large polyQ expansions form insoluble, ordered aggregates in neurons throughout the nervous system of *C. elegans* with no evidence of cell-specific solubility.

PolyQ Length-Dependent Aggregation Correlates with Neuronal Dysfunction

In human disease, and in mouse, *Drosophila*, and cell culture studies of polyQ pathogenesis, aggregation is often accompanied by cellular dysfunction, although it remains unknown whether the toxic species are polyQ aggregates visible by light microscopy or some intermediate oligomeric species along the pathway to aggregate formation.⁶² To test whether polyQ aggregation in *C. elegans* neurons was accompanied by neurotoxicity, we examined behavioral phenotypes regulated by the nervous system. The most striking phenotype was a polyQ length-dependent loss of coordinated movement leading to nearly complete paralysis. More than 60 neurons in *C. elegans* enervate muscle cells. Dysfunction or loss of these neurons results in lack of coordination or paralysis.⁶³⁻⁶⁵ Q0 or Q19 animals with no visible polyQ aggregates showed rapid movement similar to wild type (N2) animals and Q19 showed a slight decrease. Animals with visible aggregates, Q67 and Q86, had limited capacity for coordinated movement exhibiting a decrease of 85% and 89% respectively, relative to Q0 (Fig. 4). These results suggest that formation of visible polyQ aggregates correlates with neuronal dysfunction.

Unexpectedly, pan-neuronal expression of intermediate polyQ lengths, Q35 and Q40, also affected behavior. In contrast to the clear phenotypic differences observed between transgenic animals that expressed short or long polyQ proteins, individual Q35 and Q40 animals displayed heterogeneity in behavioral phenotypes (Fig. 4). These results did not seem to correlate with the soluble distribution pattern of Q35 and Q40 proteins, visually distinct from the extensive foci formation in Q67 and Q86 animals (Fig. 1E). Behavioral toxicity in intermediate animals may have resulted from aggregation in a sub-set of neurons, or Q35 and Q40 proteins may display subtle differences in biochemical state, both of which could result in neurotoxicity without overt foci formation.

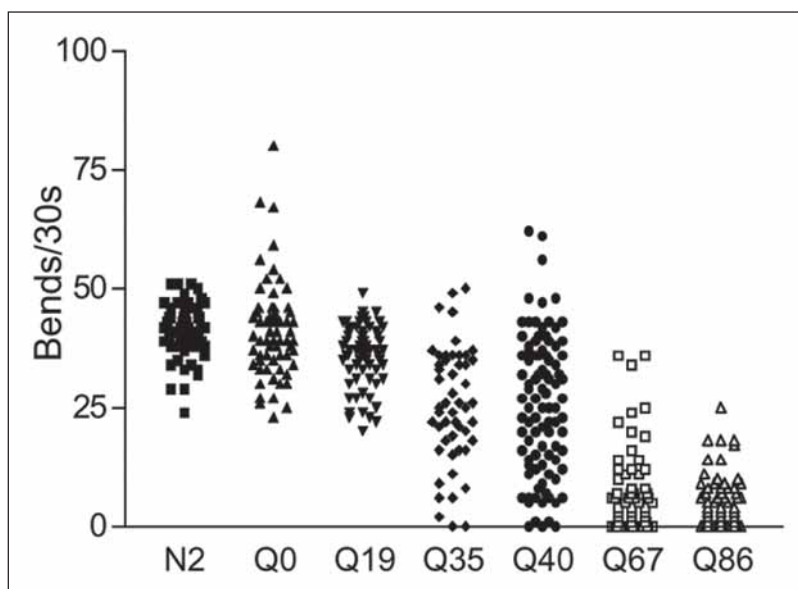


Figure 4. Increases in polyQ length correlate with neuronal dysfunction. Each point represents the average motility of a single young adult animal (4 days) over thirty seconds. Motility was quantified by determining the frequency with which animals thrashed when in liquid.¹⁰⁴

Dynamic Biophysical Properties of Intermediate polyQ Tracts in the Ventral Nerve Cord

To determine whether there was a link between behavioral phenotypes and biochemical states in Q40 animals we examined neurons associated with motility, where the most significant differences in polyQ length-dependent toxicity were observed. The highest concentration of neurons that regulate motility are found in the VNC. FRAP experiments on multiple neurons distributed throughout the VNC of a single animal reveals that Q40::YFP solubility is heterogeneous. Recovery of Q40 protein ranged from soluble, similar to Q19, or insoluble like Q86 despite the absence of overt visual foci. Areas displaying rapid, but incomplete recovery were also observed, suggesting some neurons may combine both soluble and immobile protein components. While areas of insoluble Q40 protein were observed all along the VNC, only soluble Q40 was observed in neurons in head or tail ganglia.

The heterogeneity of intermediate polyQ protein solubility led us to hypothesize that heterogeneity might also exist in the distribution pattern of Q40 proteins, although it was not detected at the resolution of our earlier microscopy studies. Upon reexamination of the visual distribution of Q40 protein at higher magnification, we found subtle yet consistent changes in distribution, with Q40::YFP proteins localized to areas of increased fluorescent intensity forming oblong shapes with well defined, tapered ends that were not observed in animals expressing either short or long polyQ expansion. Although the distribution pattern of Q40 protein localization at high magnification was distinct from other polyQ containing animals, it could not be detected under a simple dissection microscope.

To determine whether the intermediate length Q40 protein displays intermolecular interactions distinct from short (Q19) or long (Q86) polyQ proteins we performed FRET analysis. In a single young adult Q40 animal, we tested areas along the entire length of the VNC by FRAP to enable correlation of FRET results with Q40 solubility. Immediately following FRAP,

the same region was tested for FRET. In regions of where FRAP results indicate soluble Q40 protein, photobleaching of the acceptor has little effect on donor intensity suggesting that no significant Q40-Q40 protein interactions are occurring. Conversely, in regions where FRAP reveals insoluble Q40 protein, intermolecular interactions of Q40 proteins causes FRET. The efficiency of interaction for Q40 proteins reveals two distinct populations coexist within the neurons of a single Q40 animal whereas Q19 or Q86 animals display only a single type of intermolecular interaction. Together, the complementary techniques of FRET and FRAP present a profile of Q40 proteins in vivo that reveals heterogeneity of biophysical states of an intermediate-length polyQ protein which is distinct from the homogeneous states observed for long or short polyQ proteins in the neurons of a multicellular organism.

These results suggest that Q40 protein can exhibit polymorphic subcellular distribution, solubility, and intermolecular interactions in an individual animal, unlike Q86 that exhibits an invariant immobile state, consistent intermolecular interactions and consistent distribution into foci. Variable biophysical properties of Q40 protein combined with the motility assay in which behavior of individual Q40 animals ranges from wild type to severely impaired, shows that polyQ-mediated neurotoxicity in *C. elegans* can be observed in the absence of overt foci formation.

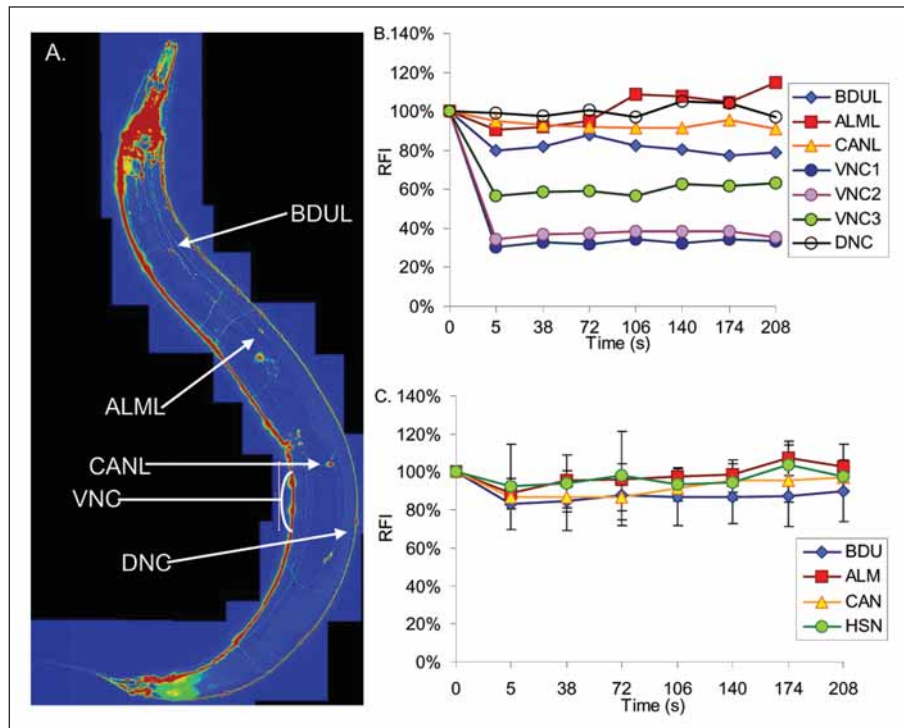


Figure 5. Solubility of polyQ proteins in specific neurons is independent of aging. A) Specific neurons are identified in the flattened z-stack of a representative Q40 animal (8 days old) and (B) FRAP results are shown for each neuron. Q40 protein in the neurons analyzed remains soluble even as animals age. C) FRAP data shown are the average for each specific neuron, with standard deviation, analyzed in animals from 4 to 8 days of age.

Neuron-Specific Responses to polyQ Proteins

Our observation that solubility of Q40 proteins in *C. elegans* can vary between different areas of the nervous system suggests that there are modifiers acting on simple polyQ proteins independent of protein context. The observed variability in polyQ protein solubility could be stochastic rather than a neuron-specific response. To address this, we performed FRAP experiments on several specific neurons in addition to the VNC. We reasoned that if solubility of Q40 protein is stochastic, protein solubility in a specific neuron will vary between animals. However, if polyQ protein solubility is neuron-specific, FRAP results should be consistent in all animals tested. FRAP analysis of specific neurons in multiple animals and show that Q40 protein is consistently soluble whereas the VNC displays polymorphic Q40 solubility in all *C. elegans* examined (Fig. 5A,B). These results suggest that polyQ solubility is consistent in specific classes of neurons. We hypothesize that polyQ solubility is modulated by some property of the neuron in which it is expressed, such as neuronal function, connectivity, activity levels, or expression levels of the polyQ protein.

Another characteristic that could have a major effect on polyQ solubility in neurons is the age of the animal. Aging is well established as a major contributor to the onset of polyQ repeat diseases in both humans and in model systems. We therefore examined specific neurons in animals of different ages show that in specific neurons, Q40 protein remains soluble in animals up to 10 days of age (Fig. 5C). In contrast, the VNC displays insoluble protein as early as three days and polymorphic solubility of Q40 persists as the animals age. These results showed that Q40 can exhibit polymorphic biochemical properties and remained soluble in some neurons while becoming aggregated in the VNC. It also suggested that some neurons displaying soluble Q40 protein are able to maintain solubility as they age. These properties of Q40 are in contrast to the complete aggregation of Q67 or Q86 proteins observed in *C. elegans* nervous system (Fig. 1) and suggest that for intermediate Q lengths, age is not the only modifier of polyQ protein solubility.

C. elegans model provides a unique tool for investigating the basis of neuron-specific toxicity associated with the expression of polyQ proteins. Behavioral and molecular characterization of polyQ expansions in a pan-neuronal system is the first step in establishing a model in which neuron-specific, novel modifiers of polyQ-mediated pathogenesis can be identified. Additionally, establishing this system in neurons provides the baseline for future studies to examine one of the major modifiers of polyQ pathogenesis: tissue type. Development of a neuronal model in *C. elegans* opens the way to comparative studies on how nonneuronal tissue, such as muscle, responds to polyQ proteins.

The *C. elegans* polyQ Series in Muscle Cells

In addition to providing a second tissue for comparative studies, *C. elegans* muscle cells have some advantages for studying the basic properties of misfolded proteins in vivo. Muscle cells are significantly larger than neurons facilitating work under comparatively low magnification. In addition, *C. elegans* muscle cells are sensitive to RNA interference (RNAi) while neurons are refractory. Therefore, a muscle cell model is ideal for rapid, genome wide screening.

Using a similar approach to that described above, fluorescently tagged polyQ proteins were expressed in muscle cells of *C. elegans*. We generated a series of transgenic animals expressing polyQ repeats of different lengths, with greater resolution at the intermediate lengths (Q0, Q19, Q29, Q33, Q35, Q40, Q44, Q64, and Q82). In young adult animals expressing repeats of Q35 or fewer, we observed diffuse fluorescence in all expressing cells while animals expressing muscle Q44, Q64 or Q82 exhibited fluorescence in discreet foci similar to that observed in neurons (Fig. 6A, Fig. 1). Muscle Q40 animals displayed a polymorphic distribution with diffuse fluorescence in some cells and foci in others, similar to neuronal Q40 but more easily observed due to the size of muscle cells. In the *C. elegans* muscle cell model, there is a shift in the cellular distribution of polyQ protein in young adult

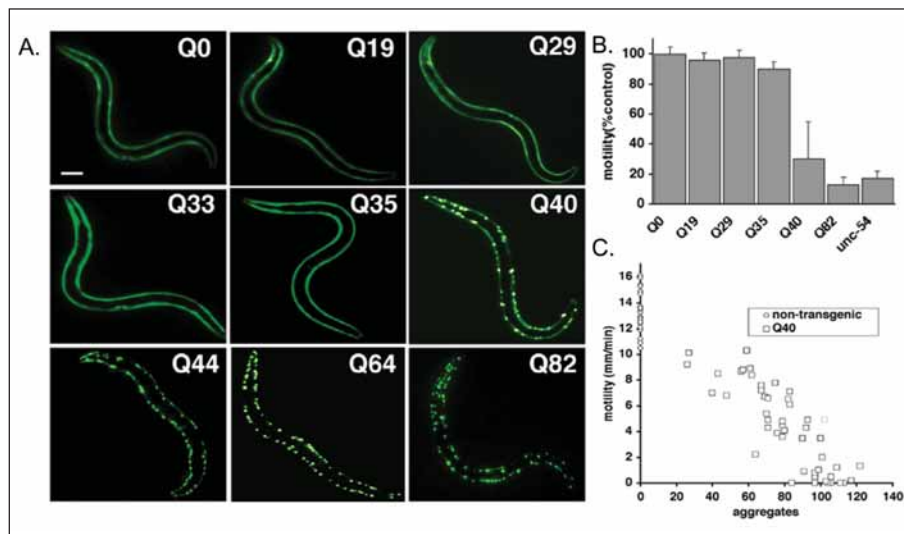


Figure 6. Expression of different polyQ::YFP lengths in *C. elegans* body-wall muscle cells shows a length-dependent aggregation phenotype. Fluorescence images of young adult *C. elegans* expressing different lengths of polyQ::YFP (Q0, Q19, Q29, Q33, Q35, Q40, Q44, Q64, Q82). Animals expressing repeats of \leq Q35::YFP show a diffuse fluorescence in all muscle cells; in contrast, animals expressing \geq Q44 repeats exhibited punctate distribution of fluorescence. Animals expressing muscle Q40 showed a polymorphic phenotype with both diffuse and punctate fluorescence distribution. (Bar = 0.1 mm). B) Quantification of motility index for young adult Q0, Q19, Q29, Q35, Q40, Q82, and *unc-54*(*r293*) animals. Data are mean \pm SD for at least 50 animals of each type as percentage of N2 motility. C) Correlation between the number of Q40 foci in the muscle cells of an individual animal and their motility.

animals between 35–40 repeats, reminiscent of the pathogenic threshold, of 30–40 repeats, observed in the human diseases.

To determine whether there is polyQ-mediated dysfunction in muscle, we examined motility and found that Q19, Q29 or Q35 animals behaved similarly to wild type (N2) while Q82 animals displayed severely decreased motility (Fig. 6B). The intermediate Q40 animals, which had aggregates in some cells but not in others, exhibited an intermediate motility defect with a high degree of variation. The polyQ-dependent motility phenotype observed in the muscle cell model was parallel to that of the neuronal model. However, the larger size of body wall muscle cells made it possible to examine how polyQ aggregation correlates with cellular dysfunction. When individual animals were assayed for motility and then scored for the number of Q40 aggregates, it became clear that in muscle cells, aggregation is directly correlated with cellular dysfunction (Fig. 6C).⁶⁶

Aging Influences the Threshold for polyQ Aggregation and Toxicity

Despite the expression of aggregation-prone proteins throughout the lifetime of the organism, pathology associated with diseases such as Huntington's, Alzheimer's and Parkinson's are typically not manifest until late in life. This motivated us to study the behavior of polyQ proteins during aging. We performed experiments in which individual Q0, Q29, Q33, Q35, Q40, and Q82 animals were examined daily for the appearance of protein aggregates and motility. Relative to Q40 and Q82 animals that quickly accumulated aggregates and exhibited a rapid decline in motility, Q33 and Q35 animals exhibited an initial lag prior to the gradual accumulation of aggregates, however to levels much lower than for Q40 or Q82

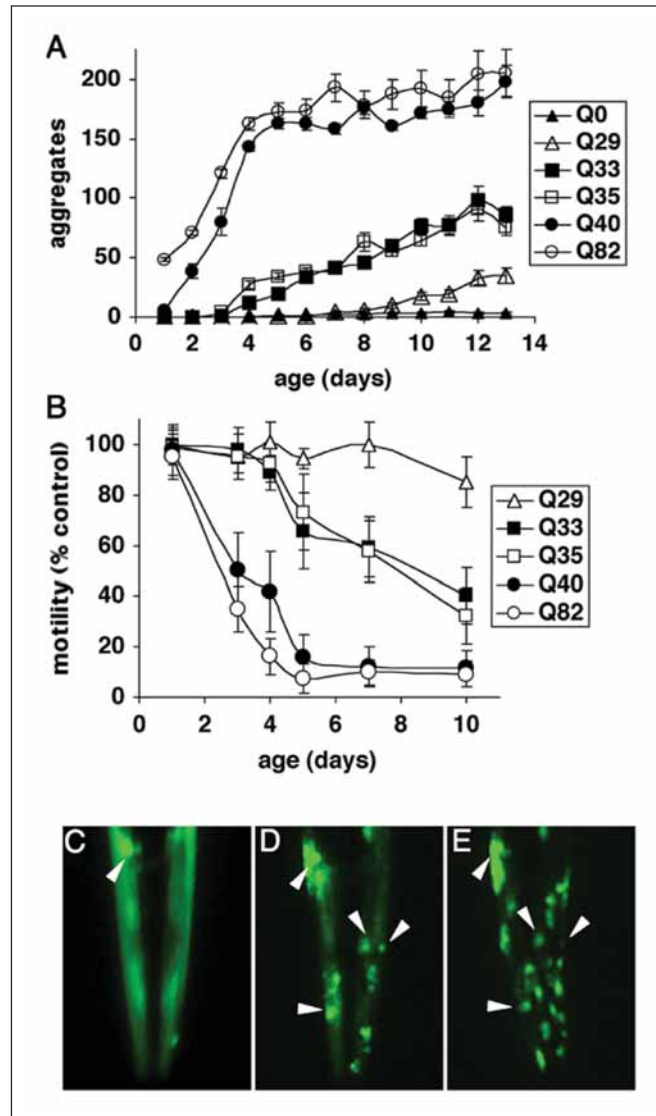


Figure 7. Influence of aging on polyQ aggregation and toxicity. A) Accumulation of aggregates in Q82, Q40, Q35, Q33, Q29, and Q0 during aging. Data are mean \pm SEM. Twenty-four animals of each type are represented at day 1. Cohort sizes decreased as animals died during the experiment, but each data point represents at least five animals. B) Motility index as a function of age for the same cohorts of animals described in A. Data are mean \pm SD as a percentage of age-matched Q0 animals. C-E) Fluorescence images of the head of an individual Q35 animal at 4 (C), 7 (D), and 10 (E) days of age, illustrating age-dependent accumulation of aggregates. Arrowheads indicate positions of the same aggregates on different days. In E, the animal is rotated slightly relative to its position in D.

(Fig. 7A). For example, aging-dependent aggregate accumulation can be readily observed by comparison of the same Q35 animal at 4, 7, and 10 days (Fig. 7C-E).

In all cases, we observed an aging-dependent loss of motility relative to controls. These results reveal that the threshold for polyQ aggregation and toxicity in *C. elegans*' muscle cells is not static, but rather age-dependent. At 3 days of age or less, only animals expressing Q40 or greater exhibit aggregates (Figs. 6, 7), whereas at 4-5 days the threshold shifts and aggregates appear in Q33 and Q35 animals (Fig. 7A). In Q29 animals, the threshold again shifts (>9-10 days) (Fig. 7). Thus, the threshold for polyQ aggregation is dynamic and likely reflects a balance of different factors including repeat length and changes in the protein folding environment.

Longevity Genes Influence Aging-Dependent Aggregation and Toxicity of polyQ Proteins

Our results reveal that the threshold for polyQ aggregation and cytotoxicity in vivo is dynamic over the lifetime of an animal. Does this dynamic behavior result from the intrinsic properties of a protein motif, or, do changes over time reflect the influence of aging-related alterations in the cell? The idea that the molecular determinants of longevity might influence

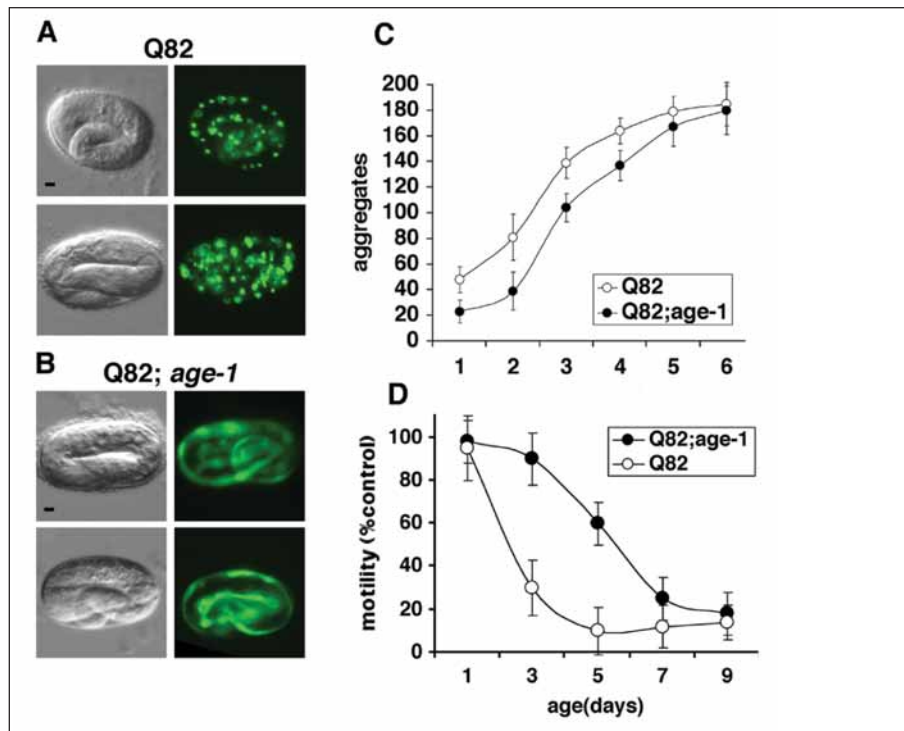


Figure 8. An extended lifespan mutation delays polyQ aggregate accumulation and onset of toxicity. A) Differential interference contrast (Left) and fluorescence (Right) micrographs showing embryos expressing Q82 in wild-type (A), *age-1(hx546)* (B) genetic backgrounds. (Bars = 5 μ m.). C) Aggregate accumulation in larval animals expressing Q40 or Q82 in the indicated genetic backgrounds relative to aggregate accumulation in wild-type background. Mean \pm SEM. D) Motility index for animals expressing Q40 or Q82 in the indicated genetic backgrounds. Data are mean \pm SEM for 30 animals of each type. Motility of nontransgenic wild-type and *age-1* animals was similar to that of wildtype (N2).

polyQ-mediated toxicity is supported by observations that the time until pathology develops - days in *C. elegans*, weeks in *Drosophila*, months in mice, and years in humans - correlates approximately with the lifespan of the organism. Here, again, the *C. elegans* model was a tremendous advantage as the availability of mutants with extended lifespans allowed us to test these ideas directly.

To accomplish this, we generated transgenic animals expressing Q82 in the background of the *age-1(hx546)* mutation or *age-1* RNAi. *age-1* encodes a phosphoinositide-3 kinase that functions in an insulin-like signaling (ILS) pathway, and mutations in this gene can extend lifespan by 1.5-2 fold.^{67,68} Q82 in the *age-1* background (Q82;*age-1*) exhibited reduced aggregate formation in embryos relative to Q82 in the wild type background (Fig. 8). Q82 aggregate formation was also reduced 30-50% during larval stages (1-2 days old) in *age-1* animals compared to wild type background and remained significantly lower through 4-5 days of age.⁶⁶ Parallel motility assays also demonstrated a delay in onset of the motility defect, consistent with slower aggregate accumulation in Q82;*age-1* animals (Fig. 8).

In wild type animals, the kinase activity of AGE-1 is required in a signaling cascade that results in constitutive repression of the fork head transcription factor DAF-16 leading to normal lifespan.^{67,69,70} Derepression of DAF-16 in *age-1* animals results in extended lifespan, and *daf-16* mutations suppress the longevity phenotype. To examine whether *age-1* effects on longevity and polyQ aggregation and toxicity are mediated through similar regulatory pathways, we tested whether *age-1* suppression of Q82 phenotypes was affected by inactivation of *daf-16* using RNAi. Q82;*age-1*; *daf-16* animals exhibited aggregation and motility phenotypes similar to Q82 expressed in wild type background. Thus, the dual effects of *age-1* on longevity and polyQ-mediated toxicity share a common genetic pathway.






Our demonstration that a mutation conferring longevity also delays polyQ aggregation and toxicity suggests a novel link between the genetic regulation of aging and aging-related disease. In subsequent studies, we and others have demonstrated that the molecular link between these pathways is regulated, in part, by factors that detect and respond to misfolded proteins - namely heat shock transcription factor (HSF) and molecular chaperones/heat shock proteins. For example, it has been shown that inhibition of HSF-1 function leads to decreased lifespan and an accelerated aging phenotype in *C. elegans*.⁷¹⁻⁷³ Conversely, overexpression of HSF-1 in *C. elegans* extends lifespan.^{72,73} Additionally, inactivation of *daf-16*, *hsf-1* or small heat shock proteins in *C. elegans* accelerated the aggregation of polyQ expansion proteins supporting the idea that ILS could coordinately influence aging and protein aggregation through the action of DAF-16, HSF-1 and molecular chaperones.

Genome-Wide RNAi Screening Identifies Novel Regulators of polyQ Aggregation and Toxicity

The results described above identify ILS as a genetic pathway that can influence the course of polyQ-mediated phenotypes. What other pathways might exert similar effects? Numerous over-expression and genetic studies in mammalian and *Drosophila* models have identified various enhancers or suppressors of polyQ-mediated aggregation and toxicity.⁷⁴⁻⁷⁶ This is well-illustrated by the large number of approaches in which various molecular chaperones either alone or in combination have been shown to influence polyQ-mediated phenotypes.^{5,7,74,76-78} While one could argue which of these modifiers is the "key" to determining the fate of aggregation-prone proteins, we interpret these results to suggest that the transition of polyQ proteins from a soluble to an aggregated state is the result of a balance in which multiple pathways are likely to cooperate. To identify the complete protein-folding buffer involved in polyQ transition from a soluble to an aggregated state we used a genome-wide RNAi approach.

RNAi is a commonly used reverse-genetics approach in *C. elegans* allowing the targeted down-regulation of specific genes by introduction of small fragments of cognate double-stranded RNAs.^{79,80} This technique has been adapted to genome-wide screens with a library consisting of 16,757 bacterial clones covering 86% of the predicted *C. elegans* genome.^{81,82} RNAi has the

Table 1. Genome-wide RNAi screen for modifiers of polyQ aggregation identified 186 genes, in five classes. These genes all function normally to suppress aggregation; therefore knockdown by RNAi resulted in increased aggregation.

↑ Production Misfolded Proteins		↓ Clearance of Misfolded Proteins		
				
RNA synthesis & processing (31) Transcription regulation (5)	Protein synthesis (59) Initiation (6)	Protein folding (11) Chaperonin (6)	Protein transport (18) Endocytosis (1)	Protein degradation (16) 19S (8)
T27F2.1 (Skip) Transcription (2)	Y39G10AR.8 (eIF-2-γ) Elongation (4)	cct-5(TCP-1-ε) Hsp70 (4)	Y105E8A.9 (γ-adaptin) Nuclear import (4)	rpt-5 (26S 6A) 20S(10)
ama-1 (RPB1) Splicing (17)	eft-3 (eEF1A-2) Ribosomal subunit (43)	hsp-1 (Hsc70) DnaJ (1)	C53D5.6 (Importin β -3) Cytoskeleton (6)	pas-4 (α type 7) Ub ligase (2)
T13H5.4 (SAP61)	rps-26 (S26)	F18C12.2A	K01G5.7 (Tubulin β -2)	C47E12.5 (E1)

additional advantages of allowing detection of lethal positives and the immediate identification of the target genes. Although genome-wide RNAi screens may miss certain genes secondary to variation in mRNA depletion and relative inefficiency of the mechanism in neurons, this approach offers an extremely powerful and rapid tool to identify the set of genes that modify a given phenotype.

To identify genes that prevent polyQ aggregate formation we used *C. elegans* strains expressing polyQ lengths close to the aggregation threshold, Q33 and Q35 strains, in an RNAi genetic screen. To validate this strategy, we first tested the full range of polyQ strains with a group of candidate modifiers, genes containing the TPR domain and therefore likely to act as molecular chaperones. Animals with knock down of candidate modifiers were analyzed for premature appearance of aggregates upon selective RNAi. Of the 72 candidate gene modifiers analyzed only four showed an earlier appearance of foci in Q33 and Q35 animals revealing an unexpected specificity among known modifiers of protein folding.⁸³ These effects were dependent on the presence of an expanded polyQ motif as no foci were observed for any of the 72 RNAi bacterial clones in either Q0 or Q24 animals. The fluorescent foci induced by RNAi-treatment were biophysically and biochemically identical to aggregates of long polyQ stretches as judged by FRAP analysis and SDS-PAGE.

Having validated the reliability of our approach, we screened the *C. elegans* genome and identified a total of 186 genes that induced earlier onset of the aggregation phenotype in Q35 animals. These modifiers fall into 5 major classes: genes involved in RNA metabolism, protein synthesis, protein folding, protein trafficking and protein degradation (Table 1). Examples of some of these genes are: RNA helicases, splicing factors and transcription factors for RNA metabolism; initiation and elongation factors and ribosomal subunits for protein synthesis; chaperonins and Hsp70 family members for protein folding; nuclear import and cytoskeletal genes for protein trafficking and proteasomal genes for protein degradation. A common feature is an expected imbalance between protein synthesis, folding and degradation triggered by their disruption. In this context, these 5 classes can then be further grouped in two major categories: genes whose disruption leads to an increase in misfolded protein production and genes that when disrupted lead to a decreased clearance of misfolded proteins and proper protein turnover. Our results reveal that the transition between soluble and

aggregated states of polyQ proteins is regulated by a much more complex integration of events, extending beyond the immediate involvement of chaperone-mediated folding and proteasomal degradation.

Our findings suggest a model in which each step in the birth, life and death of a protein influences the capacity of the cellular protein folding buffer. For example, perturbation of the RNA-processing machinery caused accelerated aggregation of Q35 perhaps due to an increased burden of abnormal proteins requiring the activity of the protein folding buffer. Uncovering the role of these genes in the disease process suggests that there may be no single molecular mechanism responsible for polyQ-mediated pathology.

Global Disruption of Folding Homeostasis by polyQ Proteins

The widespread effect of polyQ proteins leads to the question of whether polyQ proteins cause cellular dysfunction by a generalized destabilization of the cellular protein folding environment. We utilized our *C. elegans* models of polyQ aggregation in neuron or muscle cell models to examine the effect of polyQ protein on cells' ability to maintain protein-folding homeostasis. To test the hypothesis that polyQ proteins disrupt protein homeostasis, we took a genetic approach using diverse *C. elegans* temperature-sensitive (ts) mutations to examine whether their functionality at the permissive condition is affected by expression of aggregation-prone polyQ-expansions. Since many ts mutant proteins are highly dependent on the cellular folding environment they represent highly sensitive indicators of a disruption in protein homeostasis. The neuronal and muscle polyQ models described above were crossed into ts mutants to determine the effect of polyQ proteins on cellular homeostasis.⁸⁴⁻⁸⁶

Animals expressing ts mutant of the *C. elegans* homolog of a muscle paramyosin (UNC-15) were crossed to *C. elegans* polyQm strains, and phenotypes were examined at both permissive and restrictive temperature conditions. With the paramyosin ts mutation alone, animals do not display overt phenotypes at the permissive temperature, however at the restrictive temperature the ts mutation disrupts thick filament formation and leads to phenotypes including embryonic and larval lethality and slow movement in adults (Fig. 9A). In animals expressing only Q40m, neither lethality nor paralysis was observed.⁸⁷ In contrast, more than 40% of embryos coexpressing Q40m and paramyosin ts failed to hatch or move at the permissive temperature (Fig. 9B). This effect was polyQ length-dependent, because coexpression of smaller polyQ expansions with paramyosin(ts) decreased penetrance of ts phenotypes (Fig. 9B). Examination of muscle structure in paramyosin(ts) + Q40m embryos at the permissive temperature revealed a disrupted pattern of actin staining, similar to the pattern in paramyosin(ts) embryos at the restrictive temperature and absent at the permissive temperature or in wild-type animals. Thus, in muscle cells expression of an aggregation-prone polyQ protein is sufficient to cause a paramyosin ts mutation to exhibit its mutant phenotype at the permissive condition.

To determine whether this effect of polyQ expansions is specific to muscle or extends to other tissues, we examined neurons. Animals expressing a ts mutation in the neuronal protein dynamin-1 [dynamin(ts)] become paralyzed at the restrictive temperature but have normal motility at the lower, permissive temperature.⁸⁸ With the coexpression of pan-neuronal Q40, dynamin(ts) animals display severe impairment of mobility at the permissive temperature (Fig. 9C). This effect was length dependent since no phenotypes were observed in animals coexpressing the nonaggregating Q19n. Thus, expression of polyQ expansions phenocopies temperature-sensitive mutations in both muscle and neuronal cells at permissive conditions, and this genetic interaction reflects the propensity of polyQ proteins to aggregate. These observations were confirmed by testing a wide range of characterized ts mutations. Strains expressing ts mutant proteins UNC-54, UNC-52, LET-60 (*C. elegans* homologs of myosin, perlecan, and ras-1, respectively), or UNC-45 together with Q24m or Q40m were scored for specific ts phenotypes at the permissive temperature. For all lines generated, the ts mutant phenotype was exposed at permissive conditions in the presence of the aggregation prone Q40m but not by

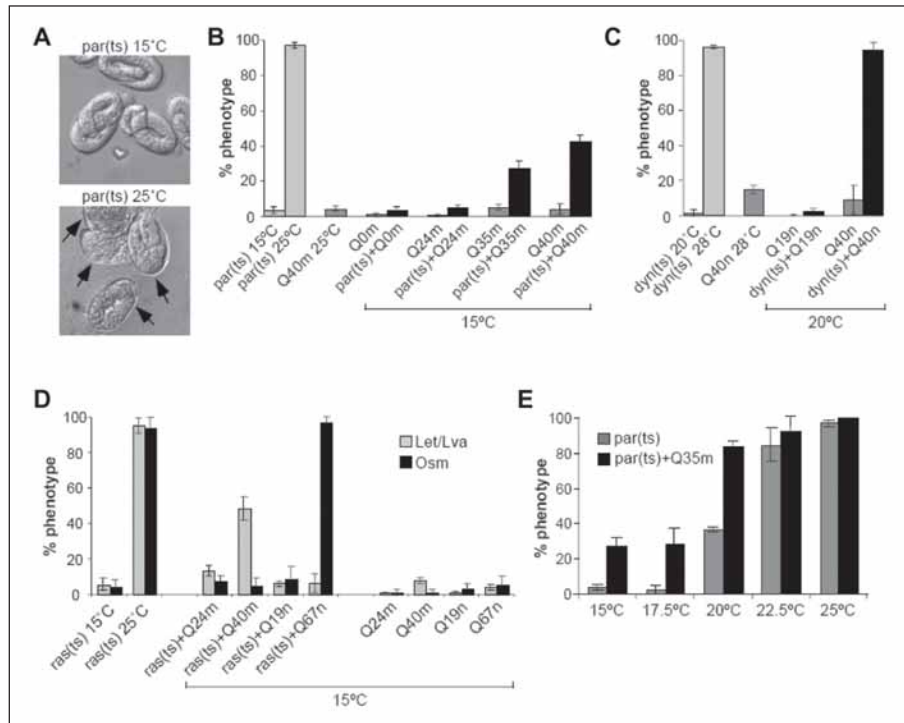


Figure 9. Aggregation-prone proteins alter the conditions required to expose phenotypes dependent on temperature sensitive mutations. Aggregation-prone proteins expose temperature sensitive phenotypes of paramyosin(ts) (B,F), dynamin(ts) (C) and ras(ts) (D) mutants at permissive temperatures. A) DIC images of age-synchronized 3-fold paramyosin(ts) embryos at indicated temperatures. Arrows indicate embryos with abnormal body shape. B) Percentage of unhatched embryos and paralyzed L1 larvae. Data are the mean \pm SD, ≥ 380 embryos per data point. C) Percentage of uncoordinated age-synchronized young adult animals. D) Percentage of animals exhibiting either Osm (black) or the combined Let/Lva (grey) phenotypes. Data are the mean \pm SD, ≥ 70 synchronized adults for Osm and ≥ 270 embryos for Let/Lva. ras(ts) + Q40m denotes ras(ts) animals heterozygous for Q40m. E) Synergistic effect of elevated temperature and polyQ expansions on paramyosin(ts). Percentage of unhatched embryos and paralyzed L1 larvae for paramyosin(ts) (grey) and paramyosin(ts)+Q35m (black) at indicated temperatures. Data are the mean \pm SD, ≥ 300 embryos for each data point. In animals expressing polyQn (neuronal)-YFP proteins (Q19n, Q40n, Q67n). Data are the mean \pm SD, ≥ 80 animals per data point.

non aggregating Q24m (Table 2). Thus, the chronic expression of an aggregation-prone polyQ protein interferes with the function of multiple structurally and functionally unrelated proteins.

The interaction between polyQ expansions and ts mutant proteins could be cell autonomous or dependent on intercellular interactions. We took advantage of tissue-specific phenotypes caused by expression of ras(ts) protein to examine this question. At the restrictive temperature, animals carrying the ras(ts) mutation display phenotypes of embryonic lethality/larval development phenotype (Let/Lva), a defect in osmoregulation (Osm) likely reflecting neuronal dysfunction and a multivulva phenotype (Muv), resulting from dysfunction in the hypodermis.⁸⁹ We scored these phenotypes upon expression of polyQ in neuronal or muscle cells. PolyQ expansions in neurons led to exposure of the Osm phenotype in ras(ts) animals at the permissive temperature but had no effect on the Let/Lva phenotype (Fig. 9D). Conversely, expression of Q40m in muscle cells of ras(ts) animals caused increased penetrance of Let/Lva

Table 2. PolyQ expansions affect the functionality of unrelated ts mutant proteins

Proteins Expressed	TS Allele	Phenotype Scored (N Value)	% Animals Displaying Phenotype			
			15°C	25°C	Q24	Q40
PolyQm	-	slow movement (n > 300)				
myosin(ts)	e1301		5.6 ± 2.6	84.7 ± 13.5	6.0 ± 5.3	4.6 ± 4.2
myosin(ts) + Qm	e1301					
myosin(ts)	e1157		5 ± 4	98.7 ± 1.4	11.2 ± 6.7	51.9 ± 19.3
myosin(ts) + Qm	e1157				5.9 ± 1.5	55 ± 6
PolyQm	-	abnormal body shape (stiff paralysis) (n > 100)			0	0
perlecan(ts)	su250		1 ± 1.2	97.6 ± 2.2	0.8 ± 1.1	48.4 ± 6.5
perlecan(ts) + Qm	su250					
PolyQm	-	egg laying defect (n > 85)			0	0
UNC-45(ts)	e286		8.4 ± 2.1	93.8 ± 4.9	5.1 ± 7.3	87.7 ± 8.1
UNC-45(ts) + Qm	e286				1 ± 0.15	7.9 ± 1.8
PolyQm	-	embryonic lethality + larval development arrest (n > 270)				
ras(ts)	ga89		5.6 ± 3.4	95.2 ± 4.3	13.3 ± 3	100*
ras(ts) + Qm	ga89					

Specific phenotype of each ts mutation alone or in polyQm background was scored at indicated temperatures. Data are the mean ± SD for at least the indicated number (n) of animals for each phenotype scored. Double homozygous ras(ts) + Q40m animals could not be scored, as they did not reach mature adulthood.

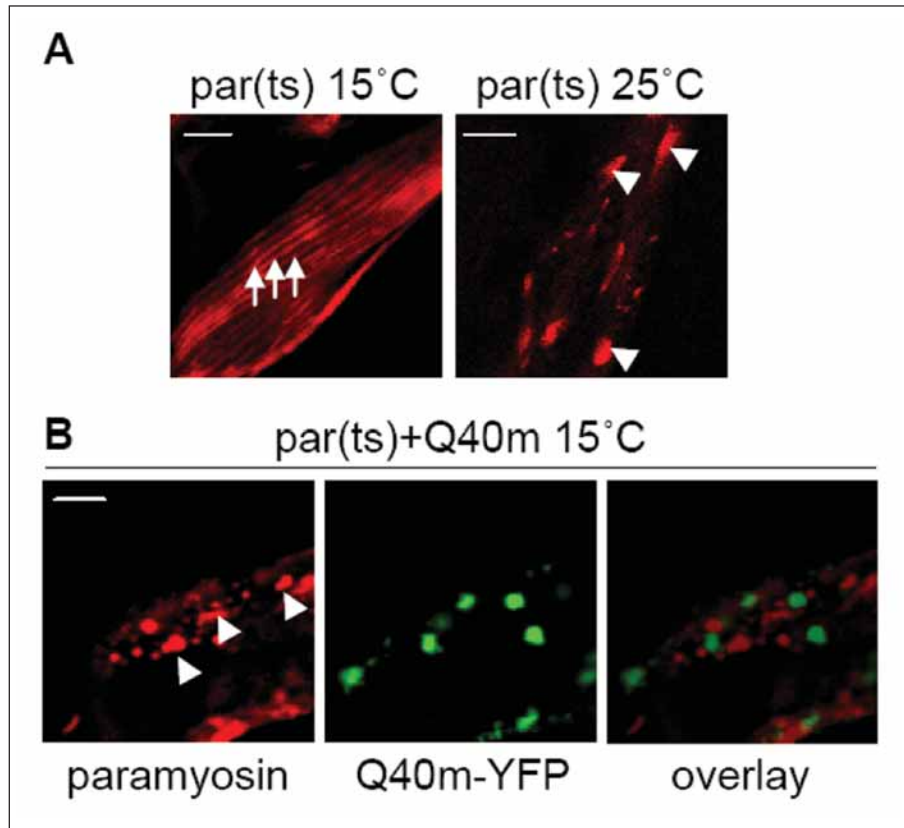


Figure 10. PolyQ expansions affect the folding of a *ts* mutant of paramyosin. A,B) Confocal images of anti-paramyosin immunostained (red) body wall muscle cells of synchronized young adults expressing indicated proteins. Arrows: normal muscle sarcomeres, arrowheads: abnormal paramyosin(*ts*) assemblies. Green color is Q40m-YFP fluorescent protein. Scale bar is 10 μ m.

phenotype but did not expose the neuronal *Osm* phenotype (Fig. 9D, Table 2). Neither neuronal nor muscle cell expression of polyQ expansions caused the hypodermal *Muv* phenotype. A similar control was performed with paramyosin(*ts*), and was not affected by polyQ expansions in neurons (Q67n). Likewise, polyQ expansions did not affect phenotypes that did not involve *ts* proteins (caused either by RNAi or gene deletion). Thus, the effect of polyQ expansions on mutant *ts* proteins reflects specific genetic interactions within the same cell type and does not result from decreased fitness of the organism.

To understand the nature of this interaction, we examined the cellular localization of paramyosin(*ts*) protein when coexpressed with Q40m. The paramyosin *ts* mutation affects protein interactions which, at restrictive temperature, results in mislocalization into foci (Fig. 10A).⁸⁷ When paramyosin(*ts*) protein is coexpressed with Q40m, it mislocalizes into foci at the permissive temperature, distinct from Q40m aggregates (Fig. 10B). Thus, expression of Q40m uncovers the protein folding defect in paramyosin(*ts*) mutant. In view of this, the differential penetrance of *ts* phenotypes (Table 2) may reflect the sensitivity of each *ts* mutation to disruption of the folding environment.

Aggregation-prone proteins may exert their destabilizing effects by placing a stress on the folding capacity of the cell. If so, additional stress, such as elevated temperature may act in

synergy with polyQ aggregates to further destabilize ts mutants. Indeed, expression of an intermediate (Q35m) expansion shifted the permissive temperature at which paramyosin(ts) was fully inactivated (Fig. 9E). Furthermore, we observed increased penetrance of ts phenotypes in homozygous Q40 animals as compared to heterozygous, consistent with the earlier onset of aggregation in homozygous Q40 animals (Table 2). If the levels of polyQ affect the folding of the ts protein, does the misfolding of the ts protein, in turn, intensify misfolding of polyQ? To answer that question, we quantified mQ40 aggregation in ts backgrounds and found that aggregation was enhanced dramatically. In contrast, mutations that cause a loss of function rather than a ts phenotype did not enhance aggregation. From a genetic perspective, temperature-sensitive mutations in proteins unrelated to cellular folding or clearance pathways behaved as modifiers of polyQ aggregation. This suggests that a positive feedback mechanism exists to enhance the disruption of cellular folding homeostasis.

The appearance of misfolded protein in the cell normally activates a stress response that increases protein refolding and turnover and thus rebalances the folding environment.^{90,91} In contrast, our results point to the unexpected sensitivity of cellular folding homeostasis to the chronic expression of misfolded proteins under physiological conditions. It is possible that the low flux of misfolded protein in conformational diseases may alone lack the capacity to activate the homeostatic stress response. This suggests that the stress response fails to compensate for the chronic expression of misfolded proteins in human disease.

One potential interpretation of our results is that the protein folding capacity of the cell, integrated at a systems level, is a reflection of expressed protein polymorphisms and random mutations,⁹² which in themselves do not lead to disease because of the balance achieved by folding and clearance mechanisms. However, these proteins may misfold and in turn contribute to the progressive disruption of the folding environment when this balance becomes overwhelmed, e.g., by the expression of an aggregation-prone protein in conformational diseases.

Conclusion

In our *C. elegans* model for the expression of isolated polyQ repeats we focused on the effects of polyQ-containing proteins in neurons or muscle cells. Expression of isolated polyQ motifs rather than full-length disease-related proteins enables us to uncover conserved features underlying a range of neurodegenerative diseases. A genome wide RNAi screen identified multiple molecular chaperones that have been implicated in polyQ diseases, as well as AD and PD. These studies have revealed a common set of factors that link the genetic regulation of protein homeostasis, stress responsiveness and longevity. Thus, longevity and fitness may be, at least in part, a consequence of the efficient detection, capture and resolution of misfolded and aggregation-prone proteins. The presence of marginally stable or folding-defective proteins in the genetic background of conformational diseases reveals potent extrinsic factors that can modify aggregation and toxicity. Given the prevalence of polymorphisms in the human genome,⁹³ the expression of metastable proteins could contribute to variability of disease onset and progression.⁹⁴ This interpretation also provides a mechanistic basis to the notion that the late onset of protein misfolding diseases may be due to gradual accumulation of damaged proteins, resulting in a compromise in folding capacity.⁹⁵ Cellular degeneration in diseases of protein conformation is unlikely to be due to a single defect. Thus, the many toxic effects on various cellular processes attributed to misfolded proteins^{7,59,96-103} could in fact be an integral part of the global disruption of protein homeostasis.

Acknowledgements

We thank members of the laboratory past and present who contributed to this work both intellectually and technically. Support for this research was provided by grants from the National Institute of General Medical Science, the National Institutes for Aging, the Huntington Disease Society of America Coalition for the Cure, and the Daniel F. and Ada L. Rice Foundation.

References

1. Kakizuka A. Protein precipitation: A common etiology in neurodegenerative disorders? *Trends Genet* 1998; 14:396-402.
2. Kopito RR, Ron D. Conformational disease. *Nat Cell Biol* 2000; 2:E207-209.
3. Stefani M, Dobson CM. Protein aggregation and aggregate toxicity: New insights into protein folding, misfolding diseases and biological evolution. *J Mol Med* 2003; 81:678-699.
4. Dobson CM. Protein folding and its links with human disease. *Biochem Soc Symp* 2001; 68:1-26.
5. Bonini NM. Chaperoning brain degeneration. *Proc Natl Acad Sci USA* 2002; 99:16407-16411.
6. Chan HY, Warrick JM, Andriola I et al. Genetic modulation of polyglutamine toxicity by protein conjugation pathways in *Drosophila*. *Hum Mol Genet* 2002; 11:2895-2904.
7. Cummings CJ, Mancini MA, Antalfy B et al. Chaperone suppression of aggregation and altered subcellular proteasome localization imply protein misfolding in SCA1. *Nat Genet* 1998; 19:148-154.
8. Kaye R, Head E, Thompson JL et al. Common structure of soluble amyloid oligomers implies common mechanism of pathogenesis. *Science* 2003; 300:486-489.
9. O'Nuallain B, Wetzel R. Conformational Abs recognizing a generic amyloid fibril epitope. *Proc Natl Acad Sci USA* 2002; 99:1485-1490.
10. Kawaguchi Y, Okamoto T, Taniwaki M et al. CAG expansions in a novel gene for Machado-Joseph disease at chromosome 14q32.1. *Nat Genet* 1994; 8:221-228.
11. Koide R, Ikeuchi T, Onodera O et al. Unstable expansion of CAG repeat in hereditary dentatorubral-pallidolusian atrophy (DRPLA). *Nat Genet* 1994; 6:9-13.
12. La Spada AR, Wilson EM, Lubahn DB et al. Androgen receptor gene mutations in X-linked spinal and bulbar muscular atrophy. *Nature* 1991; 352:77-79.
13. Orr HT, Chung MY, Banfi S et al. Expansion of an unstable trinucleotide CAG repeat in spinocerebellar ataxia type 1. *Nat Genet* 1993; 4:221-226.
14. Kamino K, Orr HT, Payami H et al. Linkage and mutational analysis of familial Alzheimer disease kindreds for the APP gene region. *Am J Hum Genet* 1992; 51:998-1014.
15. Laing NG, Siddique T. Cu/Zn superoxide dismutase gene mutations in amyotrophic lateral sclerosis: Correlation between genotype and clinical features. *J Neurol Neurosurg Psychiatry* 1997; 63:815.
16. Lucking CB, Durr A, Bonifati V et al. Association between early-onset Parkinson's disease and mutations in the parkin gene. French Parkinson's Disease Genetics Study Group. *N Engl J Med* 2000; 342:1560-1567.
17. Mizuno Y, Hattori N, Kitada T et al. Familial Parkinson's disease. Alpha-synuclein and parkin. *Adv Neurol* 2001; 86:13-21.
18. Polymeropoulos MH, Lavedan C, Leroy E et al. Mutation in the alpha-synuclein gene identified in families with Parkinson's disease. *Science* 1997; 276:2045-2047.
19. Rosen DR, Siddique T, Patterson D et al. Mutations in Cu/Zn superoxide dismutase gene are associated with familial amyotrophic lateral sclerosis. *Nature* 1993; 362:59-62.
20. Driscoll M, Gerstbrein B. Dying for a cause: Invertebrate genetics takes on human neurodegeneration. *Nat Rev Genet* 2003; 4:181-194.
21. Link CD. Transgenic invertebrate models of age-associated neurodegenerative diseases. *Mech Ageing Dev* 2001; 122:1639-1649.
22. Thompson LM, Marsh JL. Invertebrate models of neurologic disease: Insights into pathogenesis and therapy. *Curr Neurol Neurosci Rep* 2003; 3:442-448.
23. Westlund B, Stilwell G, Sluder A. Invertebrate disease models in neurotherapeutic discovery. *Curr Opin Drug Discov Devel* 2004; 7:169-178.
24. Merry DE. Animal models of Kennedy disease. *NeuroRx* 2005; 2:471-479.
25. Greene JC, Whitworth AJ, Andrews LA et al. Genetic and genomic studies of *Drosophila* parkin mutants implicate oxidative stress and innate immune responses in pathogenesis. *Hum Mol Genet* 2005; 14:799-811.
26. Greene JC, Whitworth AJ, Kuo I et al. Mitochondrial pathology and apoptotic muscle degeneration in *Drosophila* parkin mutants. *Proc Natl Acad Sci USA* 2003; 100:4078-4083.
27. Faber PW, Alter JR, MacDonald ME et al. Polyglutamine-mediated dysfunction and apoptotic death of a *Caenorhabditis elegans* sensory neuron. *Proc Natl Acad Sci USA* 1999; 96:179-184.
28. Faber PW, Voisine C, King DC et al. Glutamine/proline-rich PQE-1 proteins protect *Caenorhabditis elegans* neurons from huntingtin polyglutamine neurotoxicity. *Proc Natl Acad Sci USA* 2002; 99:17131-17136.
29. Parker JA, Connolly JB, Wellington C et al. Expanded polyglutamines in *Caenorhabditis elegans* cause axonal abnormalities and severe dysfunction of PLM mechanosensory neurons without cell death. *Proc Natl Acad Sci USA* 2001; 98:13318-13323.

30. Warrick JM, Paulson HL, Gray-Board GL et al. Expanded polyglutamine protein forms nuclear inclusions and causes neural degeneration in *Drosophila*. *Cell* 1998; 93:939-949.
31. Feany MB, Bender WW. A *Drosophila* model of Parkinson's disease. *Nature* 2000; 404:394-398.
32. Link CD. Expression of human beta-amyloid peptide in transgenic *Caenorhabditis elegans*. *Proc Natl Acad Sci USA* 1995; 92:9368-9372.
33. Oeda T, Shimohama S, Kitagawa N et al. Oxidative stress causes abnormal accumulation of familial amyotrophic lateral sclerosis-related mutant SOD1 in transgenic *Caenorhabditis elegans*. *Hum Mol Genet* 2001; 10:2013-2023.
34. Lee VM, Kenyon TK, Trojanowski JQ. Transgenic animal models of tauopathies. *Biochim Biophys Acta* 2005; 1739:251-259.
35. Marsh JL, Thompson LM. Can flies help humans treat neurodegenerative diseases? *Bioessays* 2004; 26:485-496.
36. Shulman JM, Shulman LM, Weiner WJ et al. From fruit fly to bedside: Translating lessons from *Drosophila* models of neurodegenerative disease. *Curr Opin Neurol* 2003; 16:443-449.
37. Orr HT. Beyond the Qs in the polyglutamine diseases. *Genes Dev* 2001; 15:925-932.
38. Ross CA. Polyglutamine pathogenesis: Emergence of unifying mechanisms for Huntington's disease and related disorders. *Neuron* 2002; 35:819-822.
39. Trotter Y, Lutz Y, Stevanin G et al. Polyglutamine expansion as a pathological epitope in Huntington's disease and four dominant cerebellar ataxias. *Nature* 1995; 378:403-406.
40. Zoghbi HY, Orr HT. Glutamine repeats and neurodegeneration. *Annu Rev Neurosci* 2000; 23:217-247.
41. Ross CA. When more is less: Pathogenesis of glutamine repeat neurodegenerative diseases. *Neuron* 1995; 15:493-496.
42. Margolis RL, Ross CA. Expansion explosion: New clues to the pathogenesis of repeat expansion neurodegenerative diseases. *Trends Mol Med* 2001; 7:479-482.
43. Davies SW, Turmaine M, Cozens BA et al. Formation of neuronal intranuclear inclusions underlies the neurological dysfunction in mice transgenic for the HD mutation. *Cell* 1997; 90:537-548.
44. Mangiarini L, Sathasivam K, Seller M et al. Exon 1 of the HD gene with an expanded CAG repeat is sufficient to cause a progressive neurological phenotype in transgenic mice. *Cell* 1996; 87:493-506.
45. Ordway JM, Tallaksen-Greene S, Gutekunst CA et al. Ectopically expressed CAG repeats cause intranuclear inclusions and a progressive late onset neurological phenotype in the mouse. *Cell* 1997; 91:753-763.
46. Gusella JF, MacDonald ME. Molecular genetics: Unmasking polyglutamine triggers in neurodegenerative disease. *Nat Rev Neurosci* 2000; 1:109-115.
47. Sherman MY, Muchowski PJ. Making yeast tremble: Yeast models as tools to study neurodegenerative disorders. *Neuromolecular Med* 2003; 4:133-146.
48. Andrew SE, Goldberg YP, Kremer B et al. The relationship between trinucleotide (CAG) repeat length and clinical features of Huntington's disease. *Nat Genet* 1993; 4:398-403.
49. Brinkman RR, Mezei MM, Theilmann J. The likelihood of being affected with Huntington disease by a particular age, for a specific CAG size. *Am J Hum Genet* 1997; 60:1202-1210.
50. Bargmann CI. Neurobiology of the *Caenorhabditis elegans* genome. *Science* 1998; 282:2028-2033.
51. Bargmann CI, Kaplan JM. Signal transduction in the *Caenorhabditis elegans* nervous system. *Annu Rev Neurosci* 1998; 21:279-308.
52. Brownlee DJ, Fairweather I. Exploring the neurotransmitter labyrinth in nematodes. *Trends Neurosci* 1999; 22:16-24.
53. Lippincott-Schwartz J, Patterson GH. Development and use of fluorescent protein markers in living cells. *Science* 2003; 300:87-91.
54. White J, Stelzer E. Photobleaching GFP reveals protein dynamics inside live cells. *Trends Cell Biol* 1999; 9:61-65.
55. Scherzinger E, Sittler A, Schweiger K et al. Self-assembly of polyglutamine-containing huntingtin fragments into amyloid-like fibrils: Implications for Huntington's disease pathology. *Proc Natl Acad Sci USA* 1999; 96:4604-4609.
56. DiFiglia M, Sapp E, Chase KO et al. Aggregation of huntingtin in neuronal intranuclear inclusions and dystrophic neurites in brain. *Science* 1997; 277:1990-1993.
57. Perutz MF, Johnson T, Suzuki M et al. Glutamine repeats as polar zippers: Their possible role in inherited neurodegenerative diseases. *Proc Natl Acad Sci USA* 1994; 91:5355-5358.
58. Ross CA, Poirier MA, Wanker EE et al. Polyglutamine fibrillogenesis: The pathway unfolds. *Proc Natl Acad Sci USA* 2003; 100:1-3.
59. Kim S, Nollen EA, Kitagawa K et al. Polyglutamine protein aggregates are dynamic. *Nat Cell Biol* 2002; 4:826-831.

60. Tsien RY. The green fluorescent protein. *Annu Rev Biochem* 1998; 67:509-544.
61. Berney C, Danuser G. FRET or no FRET: A quantitative comparison. *Biophys J* 2003; 84:3992-4010.
62. Ross CA, Poirier MA. Protein aggregation and neurodegenerative disease. *Nat Med* 2004; 10:S10-17.
63. White JG, Southgate E, Thomson JN et al. The Structure of the nervous system of the nematode *Caenorhabditis elegans*. *Phil Trans Royal Soc London Series B Biol Sci* 1986; 314:1-340.
64. White JG, Southgate E, Thomson JN et al. The structure of the ventral nerve cord of *Caenorhabditis elegans*. *Philos Trans R Soc Lond B Biol Sci* 1976; 275:327-348.
65. Rand JB, Nonet ML. Chapter 22. Synaptic Transmission. In: Riddle DL, Blumenthal T, Meyer BJ, Priess JR, eds. *C. elegans II*. Plainview, NY: Cold Spring Harbor Laboratory Press, 1997.
66. Morley JF, Brignull HR, Weyers JJ et al. The threshold for polyglutamine-expansion protein aggregation and cellular toxicity is dynamic and influenced by aging in *Caenorhabditis elegans*. *Proc Natl Acad Sci USA* 2002; 99:10417-10422.
67. Guarente L, Kenyon C. Genetic pathways that regulate ageing in model organisms. *Nature* 2000; 408:255-262.
68. Morris JZ, Tissenbaum HA, Ruvkun G. A phosphatidylinositol-3-OH kinase family member regulating longevity and diapause in *Caenorhabditis elegans*. *Nature* 1996; 382:536-539.
69. Lin K, Dorman JB, Rodan A et al. *daf-16*: An HNF-3/forkhead family member that can function to double the life-span of *Caenorhabditis elegans*. *Science* 1997; 278:1319-1322.
70. Ogg S, Paradis S, Gottlieb S et al. The Fork head transcription factor DAF-16 transduces insulin-like metabolic and longevity signals in *C. elegans*. *Nature* 1997; 389:994-999.
71. Garigan D, Hsu AL, Fraser AG et al. Genetic analysis of tissue aging in *Caenorhabditis elegans*: A role for heat-shock factor and bacterial proliferation. *Genetics* 2002; 161:1101-1112.
72. Hsu AL, Murphy CT, Kenyon C. Regulation of aging and age-related disease by DAF-16 and heat-shock factor. *Science* 2003; 300:1142-1145.
73. Morley JF, Morimoto RI. Regulation of longevity in *Caenorhabditis elegans* by heat shock factor and molecular chaperones. *Mol Biol Cell* 2004; 15:657-664.
74. Cummings CJ, Sun Y, Opal P et al. Over-expression of inducible HSP70 chaperone suppresses neuropathology and improves motor function in SCA1 mice. *Hum Mol Genet* 2001; 10:1511-1518.
75. Fernandez-Funez P, Nino-Rosales ML, de Gouyon B et al. Identification of genes that modify ataxin-1-induced neurodegeneration. *Nature* 2000; 408:101-106.
76. Warwick JM, Chan HY, Gray-Board GL et al. Suppression of polyglutamine-mediated neurodegeneration in *Drosophila* by the molecular chaperone HSP70. *Nat Genet* 1999; 23:425-428.
77. Carmichael J, Chatellier J, Woolfson A et al. Bacterial and yeast chaperones reduce both aggregate formation and cell death in mammalian cell models of Huntington's disease. *Proc Natl Acad Sci USA* 2000; 97:9701-9705.
78. Chai Y, Koppenhafer SL, Bonini NM et al. Analysis of the role of heat shock protein (Hsp) molecular chaperones in polyglutamine disease. *J Neurosci* 1999; 19:10338-10347.
79. Fire A, Xu S, Montgomery MK et al. Potent and specific genetic interference by double-stranded RNA in *Caenorhabditis elegans*. *Nature* 1998; 391:806-811.
80. Wang J, Barr MM. RNA interference in *Caenorhabditis elegans*. *Methods Enzymol* 2005; 392:36-55.
81. Fraser AG, Kamath RS, Zipperlen P et al. Functional genomic analysis of *C. elegans* chromosome I by systematic RNA interference. *Nature* 2000; 408:325-330.
82. Kamath RS, Fraser AG, Dong Y et al. Systematic functional analysis of the *Caenorhabditis elegans* genome using RNAi. *Nature* 2003; 421:231-237.
83. Nollen EA, Garcia SM, van Haften G et al. Genome-wide RNA interference screen identifies previously undescribed regulators of polyglutamine aggregation. *Proc Natl Acad Sci USA* 2004; 101:6403-6408.
84. Brown CR, Hong-Brown LQ, Welch WJ. Correcting temperature-sensitive protein folding defects. *J Clin Invest* 1997; 99:1432-1444.
85. Pedersen CB, Bross P, Winter VS et al. Misfolding, degradation, and aggregation of variant proteins. The molecular pathogenesis of short chain acyl-CoA dehydrogenase (SCAD) deficiency. *J Biol Chem* 2003; 278:47449-47458.
86. Van Dyk TK, Gatenby AA, LaRossa RA. Demonstration by genetic suppression of interaction of GroE products with many proteins. *Nature* 1989; 342:451-453.
87. Gengyo-Ando K, Kagawa H. Single charge change on the helical surface of the paramyosin rod dramatically disrupts thick filament assembly in *Caenorhabditis elegans*. *J Mol Biol* 1991; 219:429-441.
88. Clark SG, Shurland DL, Meyerowitz EM et al. A dynamin GTPase mutation causes a rapid and reversible temperature-inducible locomotion defect in *C. elegans*. *Proc Natl Acad Sci USA* 1997; 94:10438-10443.

89. Eisenmann DM, Kim SK. Mechanism of activation of the *Caenorhabditis elegans* ras homologue let-60 by a novel, temperature-sensitive, gain-of-function mutation. *Genetics* 1997; 146:553-565.
90. Goff SA, Goldberg AL. Production of abnormal proteins in *E. coli* stimulates transcription of lon and other heat shock genes. *Cell* 1985; 41:587-595.
91. Morimoto RI. Regulation of the heat shock transcriptional response: Cross talk between a family of heat shock factors, molecular chaperones, and negative regulators. *Genes Dev* 1998; 12:3788-3796.
92. Rutherford SL, Lindquist S. Hsp90 as a capacitor for morphological evolution. *Nature* 1998; 396:336-342.
93. Sachidanandam R, Weissman D, Schmidt SC et al. A map of human genome sequence variation containing 1.42 million single nucleotide polymorphisms. *Nature* 2001; 409:928-933.
94. Wexler NS, Lorimer J, Porter J et al. Venezuelan kindreds reveal that genetic and environmental factors modulate Huntington's disease age of onset. *Proc Natl Acad Sci USA* 2004; 101:3498-3503.
95. Oliver CN, Ahn BW, Moerman EJ et al. Age-related changes in oxidized proteins. *J Biol Chem* 1987; 262:5488-5491.
96. McCampbell A, Taylor JP, Taye AA et al. CREB-binding protein sequestration by expanded polyglutamine. *Hum Mol Genet* 2000; 9:2197-2202.
97. Muchowski PJ, Schaffar G, Sittler A et al. Hsp70 and hsp40 chaperones can inhibit self-assembly of polyglutamine proteins into amyloid-like fibrils. *Proc Natl Acad Sci USA* 2000; 97:7841-7846.
98. Perez MK, Paulson HL, Pendse SJ et al. Recruitment and the role of nuclear localization in polyglutamine-mediated aggregation. *J Cell Biol* 1998; 143:1457-1470.
99. Ii K, Ito H, Tanaka K et al. Immunocytochemical colocalization of the proteasome in ubiquitinated structures in neurodegenerative diseases and the elderly. *J Neuropathol Exp Neurol* 1997; 56:125-131.
100. Bence NF, Sampat RM, Kopito RR. Impairment of the ubiquitin-proteasome system by protein aggregation. *Science* 2001; 292:1552-1555.
101. Gabai VL, Meriin AB, Yaglom JA et al. Role of Hsp70 in regulation of stress-kinase JNK: Implications in apoptosis and aging. *FEBS Lett* 1998; 438:1-4.
102. Gu M, Gash MT, Mann VM et al. Mitochondrial defect in Huntington's disease caudate nucleus. *Ann Neurol* 1996; 39:385-389.
103. Holmberg CI, Staniszewski KE, Mensah KN et al. Inefficient degradation of truncated polyglutamine proteins by the proteasome. *EMBO J* 2004; 23:4307-4318.
104. Miller KG, Alfonso A, Nguyen M et al. A genetic selection for *Caenorhabditis elegans* synaptic transmission mutants. *Proc Natl Acad Sci USA* 1996; 93:12593-12598.